To be presented at the "Surfaces and Interfaces of Glass and Ceramics" Symposium, August 27-29, 1973
Alfred University, Alfred NY

LBL-2205

c. 1

PHASE DISTRIBUTION IN SOLID-LIQUID-VAPOR SYSTEMS

Ilhan A. Aksay, Carl E. Hoge,
and Joseph A. Pask

August 1973

Prepared for the U. S. Atomic Energy Commission
under Contract W-7405-ENG-48

For Reference

Not to be taken from this room

LAWRENCE BERKELEY LABORATORY
UNIVERSITY OF CALIFORNIA
BERKELEY

LBL-2205

DISCLAIMER

This document was prepared as an account of work sponsored by the United States Government. While this document is believed to contain correct information, neither the United States Government nor any agency thereof, nor the Regents of the University of California, nor any of their employees, makes any warranty, express or implied, or assumes any legal responsibility for the accuracy, completeness, or usefulness of any information, apparatus, product, or process disclosed, or represents that its use would not infringe privately owned rights. Reference herein to any specific commercial product, process, or service by its trade name, trademark, manufacturer, or otherwise, does not necessarily constitute or imply its endorsement, recommendation, or favoring by the United States Government or any agency thereof, or the Regents of the University of California. The views and opinions of authors expressed herein do not necessarily state or reflect those of the United States Government or any agency thereof or the Regents of the University of California.

PHASE DISTRIBUTION IN SOLID-LIQUID-VAPOR SYSTEMS

Ilhan A. Aksay, Carl E. Hoge and Joseph A. Pask

Inorganic Materials Research Division, Lawrence Berkeley Laboratory
and Department of Materials Science and Engineering,
College of Engineering; University of California,
Berkeley, California 94720

ABSTRACT

The development of microstructure in a solid-liquid-vapor system is highly dependent on the relative interfacial tensions of the phases involved. Under chemical non-equilibrium conditions, interfaces are in a state of continual change. During this transient stage, the classical Young's and the dihedral angle equations are only valid in terms of the dynamic interfacial tension values of the chemical non-equilibrium conditions. The thermodynamics of non-equilibrium conditions in a solid-liquid-vapor system are discussed. Spreading and subsequent pull-back phenomena, which are often observed in wetting studies, are successfully explained by the dynamic interfacial tension. Such phenomena play an important role in the initial particle arrangement and solution-precipitation stages of liquid phase sintering. Sessile drop experiments and permeation studies of liquids into porous compacts provide a means in understanding the nature of phase distribution in the presence of chemical non-equilibrium conditions.

I. INTRODUCTION

Spatial distribution of phases in a solid-liquid-vapor system are described by the classical Young's equation[1]

$$\gamma_{sv} - \gamma_{s\ell} = \gamma_{\ell v} \cos \theta \quad , \tag{1}$$

where γ is the interfacial tension between solid-vapor (sv), solid-liquid ($s\ell$), and liquid-vapor (ℓv) phases, $\gamma_{sv}-\gamma_{s\ell}$ is the driving force for wetting, and θ is the contact angle at a solid-liquid-vapor triple point as measured through the liquid phase. Furthermore, in systems where the solid phase is polycrystalline

$$\gamma_{ss} = 2\gamma_{sf} \cos \frac{\Phi}{2} \quad , \tag{2}$$

where γ_{ss} is the interfacial tension at the solid-solid grain boundary, γ_{sf} is either $\gamma_{s\ell}$ or γ_{sv}, and Φ is the dihedral angle[2] at a solid-fluid-solid triple point measured through the fluid phase. Both of these equations have been extensively used in various fields to describe the conditions of mechanical equilibrium of a capillary system under chemical non-equilibrium conditions, without explicitly considering the effect of chemical reactions on the interfacial tensions. Recently, it has been shown[3] that an interfacial reaction or diffusion of a component from one bulk phase to the other across an interface results in a transient decrease in the corresponding interfacial tension by an amount equal to the free energy of the effective chemical reaction per unit area at that interface. As a consequence of this transient lowering of interfacial

tension values, phenomena such as spontaneous spreading and permeation of a liquid phase along a solid-solid interface followed by a pull-back may be observed.

In this report, the thermodynamics of a solid-liquid-vapor system and the mechanics of wetting under chemical non-equilibrium conditions, based on the model of Gibbs,[4] are briefly discussed. These sections are followed with discussions on the effect of chemical reactions on phase distribution in liquid phase sintering. In the last sections, the results of some sessile drop and permeation studies in the MgO (solid) + $CaO-MgO-SiO_2-R_2O_3$ (Al_2O_3, Cr_2O_3, or Fe_2O_3) (liquid) system are discussed in order to illustrate the effect of interfacial chemical reactions on microstructure development.

II. THERMODYNAMICS OF A SOLID-LIQUID-VAPOR SYSTEM

The simple but elegant model of Gibbs[4] for surfaces has been used in the treatment of the thermodynamics of various interfacial phenomena. In this section, once again, this model is utilized to show the effect of chemical reactions on the interfacial tension.

Let us first consider a system with two homogeneous phases, α and β. The interphase between these two phases is not a two-dimensional boundary but one of finite thickness which includes the regions that are influenced by surface forces and whose properties grade into the bulk. However, for simplicity in mathematical expressions, Gibbs[4] assigned any property of the interphase to the interface, a dividing plane or surface, and assumed the bulk phases to be homogeneous and at equilibrium up to this interface. Using this approach, it can be shown[3] that the total differential, dG, of a two phase system (α and β), assuming an isothermal

and isobaric process, is

$$dG = \sum_i \mu_i^\alpha dn_i^\alpha + \sum_i \mu_i^\beta dn_i^\beta + \left(\frac{\partial G^{\alpha\beta}}{\partial A}\right) dA +$$

$$\sum_i \left(\frac{\partial G^{\alpha\beta}}{\partial n_i^\alpha}\right) dn_i^\alpha + \sum_i \left(\frac{\partial G^{\alpha\beta}}{\partial n_i^\beta}\right) dn_i^\beta + \sum_i \left(\frac{\partial G^{\alpha\beta}}{\partial n_i^{\alpha\beta}}\right) dn_i^{\alpha\beta} , \qquad (3)$$

where subscripts of the partial derivatives are omitted for brevity, μ_i^α and μ_i^β are the chemical potentials of component i in the α and β phases, and

$$\left(\partial G^{\alpha\beta}/\partial A\right)_{T,p,n_i} = \left(\partial G/\partial A\right)_{T,p,n_i} = \gamma_{\alpha\beta}$$

is the surface tension of the $\alpha\beta$ interface. The last three terms reflect the effect of compositional variations in the bulk and the interphase regions on the interfacial free energy.

The relationship between the interfacial or surface tension, $\gamma_{\alpha\beta}$, and the specific interfacial free energy, $g^{\alpha\beta}$, can be shown by expressing $\left(\partial G^{\alpha\beta}/\partial A\right)$ in terms of the surface excess Γ_i as

$$\gamma_{\alpha\beta} = \frac{\partial G^{\alpha\beta}}{\partial A} = \sum_i \left(\frac{\partial G^{\alpha\beta}}{\partial \Gamma_i}\right)\left(\frac{\partial \Gamma i}{\partial A}\right) = \sum_i \left\{ A \left(\frac{\partial g^{\alpha\beta}}{\partial \Gamma_i}\right) + \left(\frac{\partial A}{\partial \Gamma_i}\right) g^{\alpha\beta} \right\} \left(\frac{\partial \Gamma_i}{\partial A}\right) ,$$

and

$$\gamma_{\alpha\beta} = g^{\alpha\beta} - \sum_i \mu_i^{\alpha\beta} \Gamma_i \quad , \qquad (4)$$

where $\mu_i^{\alpha\beta} = \left(\partial g^{\alpha\beta}/\partial\Gamma_i\right) = \left(\partial G^{\alpha\beta}/\partial n_i\right)$ is the chemical potential of component i at the interface. At the first instant of formation of a surface by mechanical means, the composition of the surface is identical to that of the bulk; and thus, since $\sum_i \mu_i^{\alpha\beta}\,\Gamma_i = 0$, $\gamma_{\alpha\beta}^{0} = g^{0,\alpha\beta}$, where $\gamma_{\alpha\beta}^{0}$ and $g^{0,\alpha\beta}$ are the pure dynamic tension and specific free energy of the interface, respectively. With time, as adsorption takes place and the interfacial region approaches equilibrium conditions, the interfacial tension decreases[5,6] towards a static value as shown in the upper curve of Fig. 1, and it differs from the corresponding interfacial specific free energy $g^{\alpha\beta}$ as expressed in Eq. (4).

Now, the total differential of the free energy of a solid-liquid-vapor system (at constant temperature and pressure, after neglecting the effect of curvature on the pressure and assuming that the interfacial tensions are independent of orientation) is

$$dG = \sum_i \mu_i^s dn_i^s + \sum_i \mu_i^\ell dn_i^\ell + \sum_i \mu_i^v dn_i^v + \gamma_{s\ell} dA_{s\ell} + \gamma_{sv} dA_{sv} + \gamma_{\ell v} dA_{\ell v} +$$

$$\sum_{\alpha,\beta} \left\{ \sum_i \left(\frac{\partial G^{\alpha\beta}}{\partial n_i^\alpha}\right) dn_i^\alpha + \sum_i \left(\frac{\partial G^{\alpha\beta}}{\partial n_i^\beta}\right) dn_i^\beta + \sum_i \left(\frac{\partial G^{\alpha\beta}}{\partial n_i^{\alpha\beta}}\right) dn_i^{\alpha\beta} \right\} , \qquad (5)$$

where the summation $\sum_{\alpha,\beta}$ is taken over all three interfaces.

At total thermodynamic equilibrium, dG = 0; then since the variations of mass are independent of the variations of area,

$$\gamma_{s\ell} dA_{s\ell} + \gamma_{sv} dA_{sv} + \gamma_{\ell v} dA_{\ell v} = 0, \qquad (6)$$

and

$$\sum_i \mu_i^s dn_i^s + \sum_i \mu_i^\ell dn_i^\ell + \sum_i \mu_i^v dn_i^v +$$

$$\sum_{\alpha,\beta} \left\{ \sum_i \left(\frac{\partial G^{\alpha\beta}}{\partial n_i^\alpha} \right) dn_i^\alpha + \sum_i \left(\frac{\partial G^{\alpha\beta}}{\partial n_i^\beta} \right) dn_i^\beta + \sum_i \left(\frac{\partial G^{\alpha\beta}}{\partial n_i^{\alpha\beta}} \right) dn_i^{\alpha\beta} \right\} = 0. \qquad (7)$$

These two equations outline the conditions for mechanical and chemical equilibrium of the system, respectively; at this point the γ values correspond to those for static interfacial tensions. Equation (6) directly yields[4,7] Young's equation as presented in Eq. (1), when a flat and rigid solid surface is assumed, and the effect of the gravitational field and the curvature on the pressure in the liquid and the vapor is neglected. Similarly, when Eq. (6) is written in terms of ss and sℓ interfaces, the dihedral equation, Eq. (2), can be shown[8] to outline the conditions for mechanical equilibrium of a solid-fluid-solid system.

When the conditions of Eq. (7) are not satisfied throughout the system, the phases of the solid-liquid-vapor system will react with each other through the interfaces to achieve a state of chemical equilibrium. During these non-equilibrium dynamic conditions, the γ's change, and the areas change correspondingly in an effort to maintain mechanical equilibrium, as represented by Eq. (6), until dG becomes zero and the system reaches a state of chemical equilibrium. Volume changes occuring

during the reactions, if significant, will affect the physical configuration of the system.

Mass transfer across the interfaces must result in a net decrease of the free energy of the system at any time; otherwise, the reaction will not proceed. At the first instant of formation of an interface, however, only the interfacial region is involved in the chemical reaction, and thus the corresponding initial decrease in the free energy of the system is totally attributed to the decrease in the free energy of the interfacial region since the free energies of the bulk phases are not affected. The magnitude of the decrease in the specific interfacial free energy, $(-)\Delta g^{\alpha\beta}$, then is directly equal to $(-\Delta G^{\alpha\beta}/A)$. The corresponding interfacial tension is similarly reduced by an amount equal to $(-)\Delta g^{\alpha\beta}$ (Eq. (4)), as schematically shown in Fig. 1. If it is assumed that the free energy of the reaction between the phases in the interfacial region is comparable but not necessarily equal to that between the bulk phases, the value of $(-\Delta G^{\alpha\beta}/A)$ could be substantially high, and for an approximate interfacial region thickness of 20 Å, a decrease of as much as 1,000 ergs/cm^2 could be realized in the magnitude of the specific interfacial free energy and thus the interfacial tension.[3] Experimentally, negative interfacial tensions are often measured[9-11] during such chemical reactions that result in spontaneous spreading[9-17] or emulsification phenomena.[18]

Under chemical equilibrium conditions, however, specific interfacial free energies and static interfacial tensions are always positive since the bulk phases are more stable than the interfaces. Thus, after the

completion of the reaction at the interface followed by its continuation into the bulk regions by diffusion, the incremental contributions of the $\sum_i \left(\partial G^{\alpha\beta}/\partial n_i^{\alpha}\right) dn_i^{\alpha}$ and $\sum_i \left(\partial G^{\alpha\beta}/\partial n_i^{\beta}\right) dn_i^{\beta}$ terms in Eq. (5) must be such that $\gamma_{\alpha\beta}$ increases towards a static interfacial tension value. With time, the contributions of these terms will decrease and become minimal because of the decrease in the chemical potential or composition gradient from the interface into the bulk phases as they approach chemical equilibrium. Therefore, after the initial decrease, $\gamma_{\alpha\beta}$ increases and gradually approaches the static interfacial tension of the reacted bulk phases (Fig. 1), which could be higher or lower than the dynamic interfacial tension, γ^0, of the unreacted phases but should not differ from it drastically. In comparison, the top curve in Fig. 1 also shows the variation of the interfacial tension with time for a pure adsorption process.

III. MECHANICS OF WETTING UNDER CHEMICAL NON-EQUILIBRIUM CONDITIONS

Let us now consider the specific effects of several types of reactions on the solid-liquid-vapor system, assuming that chemical equilibrium exists between the vapor and the condensed phases but not between the solid and the liquid. The reactions to be considered are those that result because (i) only the solid is not saturated with some or all of the components of the liquid, (ii) only the liquid is not saturated with some or all of the components of the solid, (iii) both phases are unsaturated with respect to the other, and (iv) a compound forms at the interface.

Several dynamic stages associated with the first type of reaction are shown schematically in Fig. 2. At time t_o, Fig. 2a illustrates the instantaneous quasichemical equilibrium involving no interfacial reaction between the liquid and the solid. Young's equation (Eq. (1)) may then be expressed only in terms of the initial dynamic surface tensions. Now, as the solid solution reaction proceeds at the interface, the dynamic specific interfacial free energy, $g^{0,s\ell}$, will change by an amount $\Delta g^{s\ell}$ due to the free energy of the reaction; a corresponding change in $\gamma_{s\ell} = \gamma^o_{s\ell} + \Delta g^{s\ell}$ with time occurs, as shown in Fig. 1. When the diffusion rates of the reacting components and thus the growth rate of the reaction product are slow enough relative to the flow rate of the liquid drop, the liquid at the periphery of the drop will remain in contact with unreacted solid that has an unaltered γ^o_{sv} as long as $\Delta A_{s\ell}$ is positive; the driving force for wetting $\gamma^o_{sv} - \left(\gamma^o_{s\ell} + \Delta g^{s\ell}\right)$ which is increased by the amount $(-)\Delta g^{s\ell}$ remains constant. If the maximum driving force at t_m (Fig. 1) exceeds $\gamma_{\ell v}$, then spreading occurs;[17] and if the force does not exceed $\gamma_{\ell v}$, the contact angle continues to decrease until a transient mechanical equilibrium is reached as represented by t_1 in Fig. 2b. At this point, however, diffusion in the solid continues as shown schematically in Fig. 2c; γ^o_{sv} ahead of the liquid periphery then is also decreased by an amount $\approx (-)\Delta g^{s\ell}$.[19] The driving force for wetting therefore decreases, and the contact angle increases to a new value of θ_ε corresponding to the one for mechanical and chemical equilibria for the system (Fig. 2d). During this pull-back stage, the drop may break into isolated smaller drops if the thickness of the original drop decreases considerably during the transient spreading stage.[17]

On the other hand, when the diffusion rates of the reacting components in the solid are fast relative to the flow rate of the liquid drop,[3] both γ^{o}_{sv} and $\gamma^{o}_{s\ell}$ will simultaneously decrease by an amount $(-)\Delta g^{s\ell}$, and the liquid at the periphery of the drop will remain in contact with reacted solid, as represented schematically in Fig. 2b'. The driving force for wetting in this case does not change drastically from that due to the initial dynamic surface tensions (Fig. 2a) and remains essentially constant while the system moves to chemical equilibrium (Figs. 2b', 2c', and 2d).

Throughout these entire sequences, shown schematically in Fig. 2, the amount of material dissolved by the solid was considered to be small enough to be neglected so that the solid surface remained flat. However, if the specific volume of the solid solution phase at the interface differs appreciably from that of the unreacted solid, analysis by use of Young's equation as applied to experimentally measured contact angles could be misinterpreted because of the resulting non-existence of a flat solid surface.

Several dynamic stages associated with a reaction of type (ii), where only the liquid is not saturated with the solid, are shown schematically in Fig. 3. Figure 3a shows the configuration at t_o when the liquid phase first comes into contact with the solid and Young's equation may be used to express the conditions for mechanical equilibrium in terms of the dynamic interfacial tensions. After the initial reaction the composition of the liquid around the periphery and at the solid-liquid interface rapidly approaches equilibrium compositions relative

to the solid; correspondingly, $\gamma^{o}_{s\ell}$ and $\gamma^{o}_{\ell v}$ decrease because of the free energy contribution of the reaction, but then they rapidly approach their static interfacial tension values $\gamma_{s\ell}$ and $\gamma_{\ell v}$ (Fig. 1). During the initial reaction stage, thus, an instantaneous lowering of the contact angle or spreading may be observed[17] which is immediately followed by the drop pulling back to an equilibrium contact angle θ_{ε} which is retained until the system reaches equilibrium (Figs. 3b and 3c). With high-viscosity liquids and fast diffusion rates, however, the initial spreading may not be realized because the static interfacial tensions are attained faster than the liquid can spread. Again, as in the previous case, the amount of solid dissolved by the liquid was considered to be small enough to be neglected. In actual fact, however, as the reaction proceeds, the solid-liquid interface will drop below the solid-vapor surface,[20] complicating the analysis of mechanical equilibrium.

A type (iii) reaction is expected to be similar in behavior either to type (i) or (ii) reaction depending on whether an increase or decrease of volume of the solid occurs at the interface, but the kinetic analysis of the reaction and determination of the nature of the physical configuration become more complicated. The formation of a compound at the interface (type (iv) reaction) is also expected to cause the mechanical behavior of the system to be similar to that for one with type (i) reaction. The analysis in this case could be even more complicated, particularly if the compound should isolate the liquid from direct contact with the reacting solid.

IV. LIQUID PHASE SINTERING UNDER CHEMICAL NON-EQUILIBRIUM CONDITIONS

It has been reported[21] that liquid phase sintering kinetics can be divided into three densification stages: rearrangement, solution-precipitation, and coalescence. Upon formation of a liquid phase in a porous non-sintered compact, relative motion of particles occurs by rearrangement. If sufficient liquid is present, complete densification may occur by this process alone with the kinetics of densification being those of viscous flow.[21,22] With insufficient liquid, residual porosity remains. When the pore shape reaches a steady state configuration, the rearrangement stage is completed. Further densification must occur by another mechanism. The second stage, solution-precipitation, is characterized by a zero dihedral angle which causes liquid to penetrate along solid-solid contacts. Due to capillary pressure effects caused by porosity, a solubility gradient of the components of the solid phase in the liquid is established causing diffusion of material through the liquid. The final stage, coalescence, is characterized by the formation of a finite dihedral angle and solid-solid contacts. Densification is then due to diffusion of material through the solid phase because of the existence of a vacancy concentration gradient established by the curvature of the solid-liquid and the liquid-vapor interfaces. It can be shown, however, that in systems at bulk chemical equilibrium only two of the three proposed densification stages can be realized; i.e. when the equilibrium dihedral angle, Φ_ε, is zero only the rearrangement and the solution-precipitation stages exist, and when $\Phi_\varepsilon > o$, only the rearrangement and coalescence stages exist.

Kinetics of liquid phase sintering are determined by the relative magnitudes of the interfacial tensions and pore shapes. Compacts containing large volume fractions of liquid have no sv surfaces and form spherical porosity within the liquid phase directly upon completion of the rearrangement stage. On the other hand, compacts with insufficient liquid normally have sv surfaces and form toroidal shaped porosity after the rearrangement stage; as solution-precipitation proceeds, liquid is squeezed into the void space, and eventually spherical porosity forms.

Therefore, if one defines a stage in sintering as an interval during which the pore shape remains constant, as well as an interval during which the sintering mechanism remains constant, there are clearly two stages of solution-precipitation for compacts containing small liquid volumes. The first stage is characterized by toroidal shaped porosity, and the second stage is characterized by the presence of spherical porosity.

Kingery[21] has presented a kinetic analysis for the second stage of solution-precipitation. His method has been extended by Hoge and Pask[23] to describe the kinetics of both stages of solution-precipitation. Results for densification as a function of time and the initial volume are given in Table I.

If $\gamma_{ss} < 2\gamma_{s\ell}$, an equilibrium dihedral angle greater than zero degrees and solid-solid contacts are formed. Under these conditions solution-precipitation can cause surface rearrangement, but does not lead to densification. Sintering kinetics are then characterized by solid state diffusion mechanisms, either bulk or grain boundary.

However, the liquid as well as the magnitude of the dihedral angle affect the sintering kinetics. Hoge and Pask[23] have presented a kinetic analysis for the non-zero dihedral angle case, corresponding to small liquid volumes and bulk diffusion. The values of the time exponent, x, are given in Table I for several ratios of $\gamma_{s\ell}/\gamma_{\ell v}$. An analysis for grain boundary diffusion has been given by Gessinger, et al.[24]

All kinetic analyses discussed above assume static interfacial tensions. In real compacts, interfacial tensions initially change continuously, as do corresponding dihedral angles, as the system moves to chemical equilibrium. Under such conditions, the dihedral angle equation, Eq. (2), is only valid in terms of the dynamic interfacial tensions.

Let us now, as in the previous section, consider the specific effects of several types of chemical reactions on the dihedral angle, assuming that chemical equilibrium exists between the vapor and the condensed phases but not between the solid and the liquid. The first type of reaction corresponds to the case where only the solid is not saturated with some or all of the components of the liquid. Two dynamic sequences associated with this type of reaction are shown schematically in Fig. 4. Let us assume firstly that the diffusion rates of the reacting components in the solid are slow compared to the penetration rate of the liquid along the solid-solid interface. Under these conditions, the solid-liquid interfacial tension is reduced by the free energy of the interfacial reaction (Section II), but γ^{o}_{ss} is unaffected since the reaction product has not moved ahead of the triple point. Thus, if the contribution of the interfacial reaction is large enough in magnitude, the

reduction in the solid-liquid interfacial tension can be sufficiently large to cause a dynamic zero dihedral angle, as shown in Fig. 4a. At this instant, it is thermodynamically favorable for the solid-solid interface to be replaced by two solid-liquid interfaces. As this happens, the liquid is continuously exposed to an unreacted solid-solid interface and continues to penetrate it.

On the other hand, when the diffusion rates of the reacting components in the solid are fast relative to the penetration rate of the liquid along the solid-solid interface, both $\gamma^{o}_{s\ell}$ and γ^{o}_{ss} are affected simultaneously by the interfacial chemical reaction. Thus, the combined reduction of $\gamma^{o}_{s\ell}$ and γ^{o}_{ss} by the interfacial reactions can cause the dihedral angle to be relatively unaffected by the reaction, resulting in a finite dihedral angle as the system moves to chemical equilibrium, as shown in Fig. 4b.

During these reaction stages, if the sintering compact contains very small amounts of liquid relative to the solid, complete dissolution of the liquid in the bulk solid can result as the interfacial reaction continues, causing the liquid to be entirely eliminated. At this point, a finite dihedral angle, determined by the resulting γ_{sv} and γ_{ss}, would appear. On the other hand, if the amount of material going into solid solution is large, volume changes of the solid also have to be considered in the analysis.

The second type of reaction corresponds to the case where only the liquid is not saturated with the solid and dissolution of the solid occurs until the liquid is saturated. The dissolution reaction at the solid-liquid interface causes $\gamma_{s\ell}$ to be reduced instantaneously relative

to γ_{ss}, which in turn causes the dihedral angle to be lowered for a transient period. In this stage, the penetration of the liquid along the solid-solid interface is further aided by the preferential dissolution of the solid at the grain boundaries if they are poorly formed and thus are high energy sites. Liquid then will tend to penetrate the grain boundaries as long as the liquid is unsaturated with the solid. Upon saturation, the equilibrium dihedral angle will form, recreating solid-solid contacts, and possibly trapping liquid in isolated pockets.

When both phases are unsaturated with respect to the other, the dynamic reaction stages are similar in behavior to either one of the above reaction types depending on whether an increase or decrease of the volume of the solid occurs at the interface. If a compound forms due to interfacial reactions, the mechanisms are similar to those for the first type of reaction.

It was stated earlier that the magnitude of the dihedral angle determines the sintering mechanism and influences the sintering kinetics. In the absence of bulk chemical reactions, after the initial viscous flow rearrangement, the densification kinetics will be either those of solution-precipitation (zero dihedral angle) or those of solid phase sintering in the presence of a liquid phase (non zero dihedral angle), Table I. In the presence of chemical reactions, however, a transient penetration of the liquid along the solid-solid boundary may occur in all of the chemical non-equilibrium cases discussed above. All three densification stages can then be realized as the system approaches chemical equilibrium. As shown in Table I, the sintering kinetics will differ markedly during this process. During the coalescence stage, however,

the effect of interfacial reactions on the $\gamma_{s\ell}/\gamma_{\ell v}$, and thus the sintering kinetics, is not significant since for practical purposes, the time exponent, x, is not appreciably affected by the $\gamma_{s\ell}/\gamma_{\ell v}$ ratio, Table I.

V. WETTING OF MAGNESIUM OXIDE

Wetting of magnesium oxide by $CaO-MgO-SiO_2-R_2O_3$ (Al_2O_3, Cr_2O_3, or Fe_2O_3) liquids has been studied by Aksay, et al.[17] Experiments to be discussed and evaluated were performed at 1550° in air on cleaved (001) surfaces of MgO single crystals. The liquid of monticellite, $CaO \cdot MgO \cdot SiO_2$ (CMS), composition is in equilibrium with MgO after a slight precipitation of MgO in the CMS liquid.[25] The CMS-MgO equilibrium, however, is disturbed with the addition of Al_2O_3, Cr_2O_3, or Fe_2O_3. The solubilities[26] of Al_2O_3, Cr_2O_3, and Fe_2O_3 (FeO) in MgO are <0.5, 9.0, and 51.0 wt%, respectively. The interfacial reaction to consider between the liquid and the solid is

$$MgO_{(s)} + R_2O_3 \text{ (in liquid)} \rightarrow MgR_2O_4 \text{ (in MgO)}, \tag{8}$$

which results in the formation of an MgO solution with MgR_2O_4. At 1823K, an average value for the standard free energy of this reaction,[27] ΔG°, is -8,000 cal/mol. The free energy of the reaction (8), then, is

$$\Delta G = RT \ln \frac{a_{MgR_2O_4}}{a_{R_2O_3}} - 8{,}000 , \tag{9}$$

where R is the gas constant, T is the absolute temperature, and a is the activity of the designated component. Assuming that Raoult's law is applicable, $a_{MgR_2O_4}$ is equal to the concentration of MgR_2O_4 in the MgR_2O_4 solid solution at equilibrium with the MgO solid solution. A typical value[26] for $a_{MgR_2O_4}$ is ≈ 0.9. Similarly, $a_{R_2O_3}$ depends on the concentration of R_2O_3 in the liquid phase. Assuming a value of 0.5 for $a_{R_2O_3}$, $\Delta G = -6{,}050$ cal/mol, and the corresponding transient reduction in the solid-liquid interfacial tension could be as high as 1,000 dynes/cm.[3] As the concentration of R_2O_3 in the liquid increases and the liquid becomes saturated with respect to MgR_2O_4, a second possible interfacial reaction is

$$MgO\ (\text{sat. with } MgR_2O_4) + R_2O_3\ (\text{in liquid}) \rightarrow MgR_2O_4\ (\text{sat. with } MgO) \quad (10)$$

which results in the formation of a spinel compound at the interface. The contribution of the free energy of this reaction to the reduction of any of the interfacial energies, however, is zero since all the phases involved in the reaction are at equilibrium with each other. The interfacial reaction (10) does not contribute to additional changes in $\gamma^o_{s\ell}$ other than the changes due to the precurser reaction (8).

As pointed out in Section III, in addition to the contribution of the interfacial reaction on $\gamma^o_{s\ell}$, one also has to consider the kinetics of the growth of the reaction product relative to the flow rate of the liquid drop in order to determine if γ^o_{sv} will simultaneously be affected by the same reaction. Diffusion kinetics of Al^{3+}, Cr^{3+}, and Fe^{3+} in bulk MgO have been reported. At 1550°C, the volume diffusivities of

Al^{3+} and Fe^{3+} in MgO are 1.6×10^{-9} and 9.55×10^{-9} cm^2/sec, respectively,[28,29] whereas the diffusivity of Cr^{3+} is 6.6×10^{-12} cm^2/sec.[30] Assuming that the surface diffusivities, D_S, of these cations in MgO are proportional to the volume diffusivities, $D_S^{Cr^{3+}} \ll D_S^{Al^{3+}}$ and $D_S^{Fe^{3+}}$. The growth rate of the MgO ($MgCr_2O_4$) solution at the interface, therefore, is expected to be considerably slower than the growth rate of the MgO($MgAl_2O_4$) or MgO($MgFe_2O_3$) solid solution.[3,17]

The results of the sessile drop experiments as shown in Fig. 5 support the above discussion. Liquids with Cr_2O_3 additions in excess of 3 wt% showed spreading for periods of up to 6 h. With Al_2O_3 and Fe_2O_3 additions, the contact angle was lowered but no spreading took place. The microstructure studies[17] showed the growth of the MgO ($MgAl_2O_4$) and MgO ($MgFe_2O_3$) solid solutions into the sv interface as schematically shown in Fig. 2b'. The contact angle values of Fig. 5 for Al_2O_3 and Fe_2O_3 additions correspond, essentially, to the equilibrium values, θ_ε, Fig. 2d. The liquids with Cr_2O_3 additions spread since the growth rate of the solid solution product is slower than the spreading rate of the liquid drop and thus the driving force for wetting, as shown in Fig. 2b, is high due to an unaffected γ_{sv}^o. When the experiments with Cr_2O_3 additions, however, were repeated with much smaller drops and larger substrates, the spreading drop did not reach the edges of the substrate. The drops with 3.0 and 5.0 wt% Cr_2O_3 additions showed some recession from the periphery of furthest spreading and formed contact angles of 7° and 6°. This effect would be expected when the Cr_2O_3 content in the liquid is reduced resulting in a substantial reduction of the ΔG of

reaction (8), Eq. (9). Similarly, the drop with 15 wt% Cr_2O_3 initially spread and segregated into small segments and droplets as it tried to pull back when the ΔG of reaction (8) was reduced.

VI. PERMEATION OF SILICATES INTO MAGNESIA

The permeation of the CMS-R_2O_3 liquids of the previous section into sintered MgO compacts of 92.5% of the theoretical density and 3.1% open porosity has been studied by Wong.[8] The experiments were performed at 1550°C for periods of 5 min to 2 h. The permeation distance of the liquids into the compacts as a function of the annealing time at temperature is shown in Fig. 6. Since the penetration rate of a liquid along a capillary is directly proportional to the square root of $(\gamma_{sv}-\gamma_{s\ell})$,[3] the direct correlation between the contact angles of the previous section and the penetration kinetic data shown in Fig. 6 then is in agreement with the capillary penetration theory.[31]

A more important aspect of these studies, however, is that the microstructures developed after the liquid permeation into the MgO compact were in direct support of the discussions of Section IV. Figure 7 shows the microstructure of an MgO compact permeated by a liquid containing 15 wt% Cr_2O_3 after 5 min at 1550°C. A thin film of liquid is present along most of the grain boundaries although the reported[32] equilibrium dihedral angle for the system is 45°. Since the solid-solid contacts existed[8] prior to the permeation of the liquid, the complete penetration of the liquid along the solid-solid grains is explained by the transient reduction of the $\gamma_{s\ell}$ during chemical reactions, Fig. 4a.

No permeation of the liquids with high Fe_2O_3 additions (45.0 and 55.0 wt% Fe_2O_3) was observed although the liquid with 5.0 wt% Fe_2O_3 addition permeated the MgO compacts as expected on the basis of the corresponding contact angle value (Figs. 5 and 6). The microstructure shown in Fig. 8 shows the MgO-liquid interface of a permeation couple with a liquid composition of 45 wt% Fe_2O_3 after 2 h at 1550°C. The lack of permeation into MgO is clearly explained by the closing off of the channels at the interface due to the extensive volume increase with the formation of MgO ($MgFe_2O_4$) solid solution. $MgFe_2O_4$ precipitation (white particles) took place during cooling of the specimen. Any liquid that may have permeated into the compact before the channels were closed off probably disappeared as it reacted with the solid to form solid solution.

VII. SUMMARY

Under bulk chemical equilibrium conditions, Young's and dihedral angle equations in terms of the static interfacial tensions outline the condition of mechanical equilibrium in a solid-liquid-vapor system. Under bulk chemical non-equilibrium conditions, mass transfer across an interface results in a transient decrease in the corresponding interfacial free energy and thus the interfacial tension by an amount equal to the free energy of the effective chemical reaction per area at that interface. When the chemical reaction is between the solid and the liquid, in sessile drop experiments, a transient lowering of the contact angle or spreading is observed if the growth rate of the reaction product is slower than the spreading rate of the liquid. Similarly, in a solid-liquid-solid system, in the presence of chemical reactions, a transient

penetration of the liquid along the solid-solid boundary may occur. This transient stage then corresponds to the solution-precipitation stage of liquid phase sintering in systems that are characterized with equilibrium non-zero dihedral angles.

ACKNOWLEDGMENT

This work was supported by the United States Atomic Energy Commission.

REFERENCES

1. T. Young, Phil. Trans. Roy. Soc. London 95, 65 (1805).

2. C. S. Smith, Trans. AIME 175, 15 (1948).

3. I. A. Aksay, C. E. Hoge, and J. A. Pask, "Thermodynamics of Wetting" submitted to J. Appl. Phys.

4. J. W. Gibbs, Trans. Conn. Acad. 3, 343 (1878); also included in Scientific Papers of J. W. Gibbs (Dover Publ., Inc., New York, 1961) Vol. 1.

5. R. Defay, I. Prigogine, A. Bellemans, and D. H. Everett, Surface Tension and Adsorption (John Wiley and Sons, Inc., New York, 1966).

6. D. A. Netzel, G. Hoch, and T. I. Marx, J. Colloid Sci. 19, 774 (1964).

7. R. E. Johnson, Jr., J. Phys. Chem. 63, 1655 (1959).

8. B. Wong, "Permeation of Silicate Liquids into Sintered Magnesia Compacts," (M.S. Thesis) LBL-877, University of California, Berkeley, August 1972.

9. A. A. Leont'eva, Koll. Zhurn. 11, 176 (1949).

10. P. Kozakevitch, G. Urbain, and M. Sage, Rev. Met. 52, 161 (1955).

11. S. I. Popel, O. A. Esin, G. F. Konovalov, and N. S. Smirnov, Dokl. Akad. Nauk SSSR 112, 104 (1957), or Proc. Acad. Sci. USSR - Phys. Chem. 112, 27 (1957).

12. M. Humenik, Jr. and W. D. Kingery, J. Am. Ceram. Soc. 37, 18 (1954).

13. W. M. Armstrong, A. C. D. Chaklader, and M. L. A. DeCleene, J. Am. Ceram. Soc. 45, 407 (1962); W. M. Armstrong, A. C. D. Chaklader, and D. J. Rose, Trans. AIME 227, 1109 (1963); and A. C. D. Chaklader, W. M. Armstrong, and S. K. Misra, J. Am. Ceram. Soc. 51, 630 (1968).

14. A. A. Zhukhovitskii, V. A. Grigorian, and E. Mikhalik, Dokl. Akad. Nauk SSSR 155, 392 (1964), or Proc. Acad. Sci. USSR - Phys. Chem. 155, 255 (1964).

15. J. E. McDonald and J. G. Eberhart, Trans. AIME 233, 512 (1965).

16. V. I. Kostikov and B. S. Mitin, Sb., Mosk. Inst. Stali Splavov, No. 49, 114 (1968).

17. İ. A. Aksay, A. P. Râju, and J. A. Pask, "Wetting of Magnesium Oxide by Silicate Liquids," submitted to J. Am. Ceram. Soc.

18. J. T. Davies and E. K. Rideal, Interfacial Phenomena (Academic Press, New York, 1963), 2nd ed., p. 360.

19. The free energy change at the solid-vapor interface is designated as $\Delta g^{s\ell}$ instead of Δg^{sv} since, assuming that composition of the liquid at the interface remains essentially constant, compositional variations are only in the solid due to components diffusing from the liquid and thus the nature of the reactions at the solid-vapor and the solid-liquid interfaces do not differ appreciably.

20. R. D. Carnahan, T. L. Johnston, and C. H. Li, J. Am. Ceram. Soc. 41, 343 (1958); and J. A. Champion, B. J. Keene, and J. M. Sillwood, J. Mater. Sci. 4, 39 (1969).

21. W. D. Kingery, J. Appl. Phys. 30, 301 (1959).

22. J. Frenkel, Zhur. Tech. Fiz. 9, 305 (1945), or J. Phys. (USSR) 9, 385 (1945); and F. V. Lenel, The Physics of Powder Metallurgy, W. E. Kingston, ed. (McGraw-Hill Book Company, New York, 1951), p. 238.

23. C. E. Hoge and J. A. Pask, "Kinetics of Liquid Phase Sintering," unpublished.

24. G. H. Gessinger, H. F. Fischmeister, and H. L. Lukas, Acta Met. 21, 715 (1973).

25. E. F. Osborn and A. Muan, Phase Diagrams for Ceramists, E. M. Levin, C. R. Robbins, and H. F. McMurdie, eds. (The Am. Ceram. Soc., Inc., Columbus, Ohio, 1964), p. 210, Fig. 598.

26. A. M. Alper, R. N. McNally, P. H. Ribbe, and R.C. Doman, J. Am. Ceram. Soc. 45, 263 (1962); A. M. Alper, R. N. McNally, R. C. Doman, and F. G. Keihn, J. Am. Ceram. Soc. 47, 30 (1964); and J. C. Willshee and J. White, Trans. Brit. Ceram. Soc. 66, 541 (1967).

27. A. Navrotsky and O. J. Kleppa, J. Inorg. Nucl. Chem. 30, 479 (1968).

28. W. P. Whitney, II, and V. S. Stubican, J. Phys. Chem. Solids 32, 305 (1971).

29. S. L. Blank and J. A. Pask, J. Am. Ceram. Soc. 52, (1969).

30. H. Tagai, S. Iwai, T. Iseki, and M. S. Tokio, Radex-Rundschau 4, 577 (1965).

31. E. W. Washburn, Phys. Rev. 17, 273 and 374 (1921).

32. B. Jackson, W. F. Ford, and J. White, Trans. Brit. Ceram. Soc. 62 577 (1963); and B. Jackson and W. F. Ford, Trans. Brit. Ceram. Soc. 65, 19 (1966).

Table I. Values of the time (t) exponent, x, in $(\Delta V/V_o) \sim t^x$ for various densification stages of liquid phase sintering. V_o denotes the original volume

Densification Stage	Time Exponent, x
Rearrangement (viscous flow[21,22])	1.50
Solution precipitation:	
Initial stage	0.24
Final stage	0.36
Coalescence (solid phase sintering in the presence of a liquid phase):	
$\gamma_{s\ell}/\gamma_{\ell v} = 0.05$	0.437
$\gamma_{s\ell}/\gamma_{\ell v} = 1.0$	0.464
$\gamma_{s\ell}/\gamma_{\ell v} = 2.0$	0.471
$\gamma_{s\ell}/\gamma_{\ell v} = 3.0$	0.475

FIGURE CAPTIONS

Fig. 1. Variation of dynamic interfacial tension with time during a chemical reaction between two phases. The degree of minimization of the interfacial tension at t_m is proportional to $\Delta g^{\alpha\beta}$. In case of a pure adsorption process, no minimum is observed (top curve).[3]

Fig. 2. Schematic representation of the various dynamic stages of a sessile drop when the initial solid is not saturated with some or all of the components of the liquid. The path "abcd" corresponds to the case where the growth rate of the reaction product is slower than the flow rate of the liquid drop; and path "ab'c'd" corresponds to the case where the growth rate of the reaction product is faster than the flow rate of the liquid drop.[3]

Fig. 3. Schematic representation of the dynamic stages of a sessile drop when the initial liquid is not saturated with some or all of the components of the solid.

Fig. 4. Schematic representation of the two dynamic stages of a solid-liquid-solid system when the solid is not saturated with some or all of the components of the liquid and when the growth rate of the reaction product is (a) slower and (b) faster than the penetration rate of the liquid along the solid-solid interface.[3]

Fig. 5. The effect of R_2O_3 additions to monticellite liquid on contact angle, after 3 h at 1550°C.[17]

Fig. 6. The permeation distance of the $CaO-MgO-SiO_2-R_2O_3$ liquids into MgO compacts as a function of time at 1550°C.[8]

Fig. 7. The microstructure of an MgO compact after permeated by a liquid of 15 wt% Cr_2O_3 + 85 wt% $CaO \cdot MgO \cdot SiO_2$ composition for 5 min at 1550°C.[8]

Fig. 8. The microstructure of the solid-liquid interface of an MgO-liquid permeation specimen with an original liquid composition of 45 wt% Fe_2O_3 + 55 wt% $CaO \cdot MgO \cdot SiO_2$ after 2 h at 1550°C.[8]

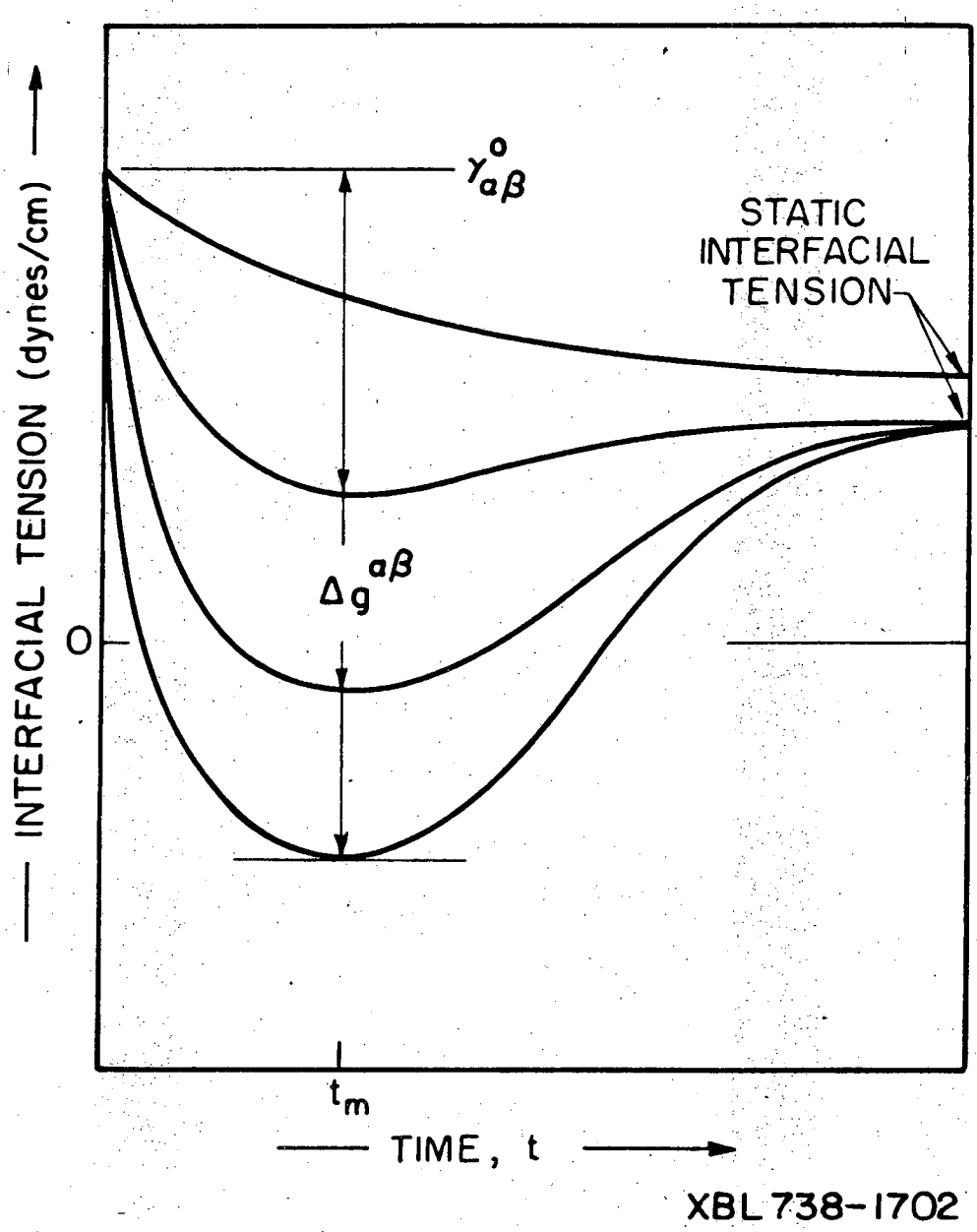
$\gamma^{o}_{\alpha\beta}$
STATIC
INTERFACIAL
TENSION
$\Delta g^{\alpha\beta}$
0
INTERFACIAL TENSION (dynes/cm)
t_m
TIME, t
XBL 738-1702

Fig. 1

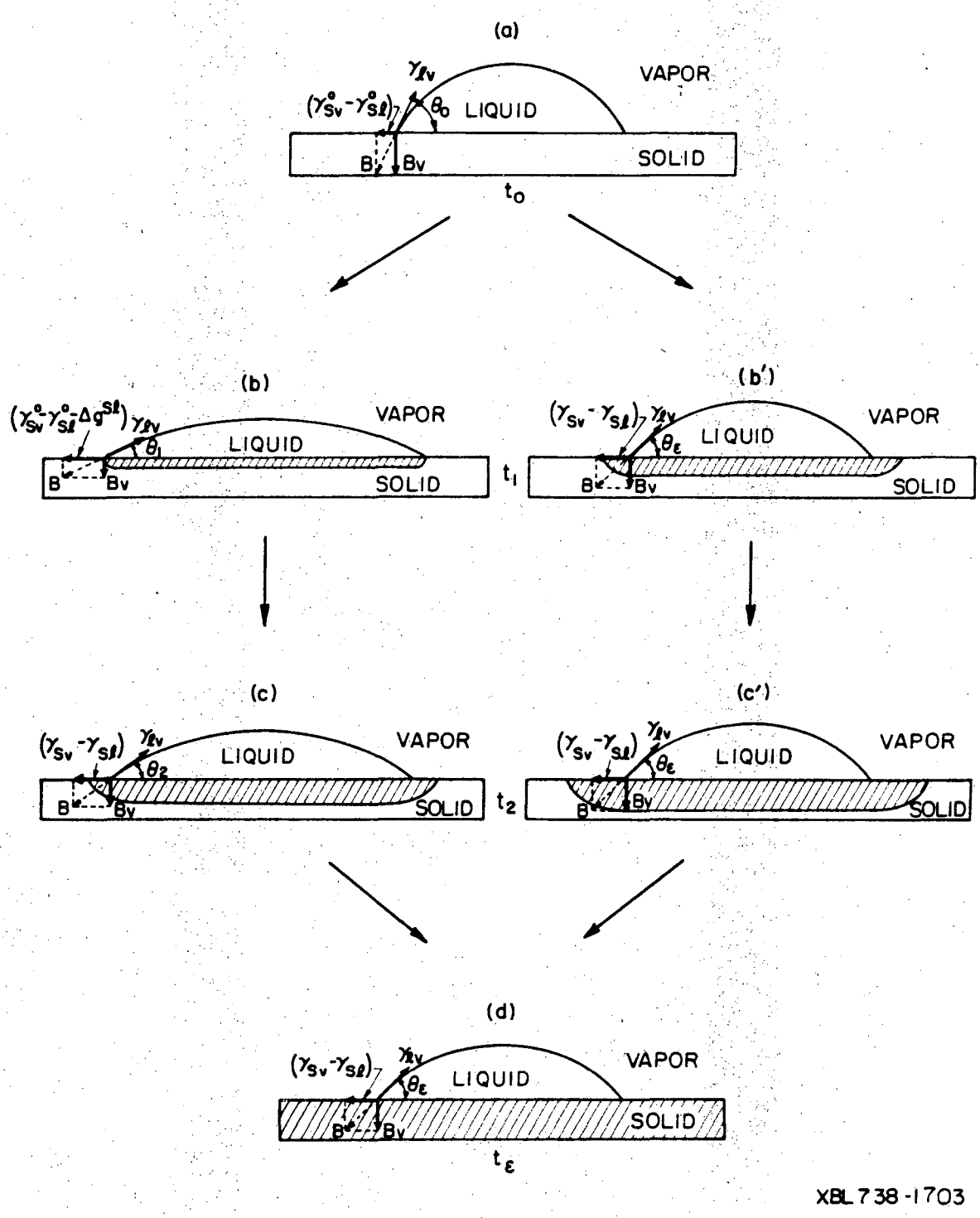
(a)
VAPOR
LIQUID
SOLID
B
Bv
t_0
(b)
VAPOR
LIQUID
SOLID
B
Bv
t_1
(b')
VAPOR
LIQUID
SOLID
B
Bv
(c)
VAPOR
LIQUID
SOLID
B
Bv
t_2
(c')
VAPOR
LIQUID
SOLID
B
Bv
(d)
VAPOR
LIQUID
SOLID
B
Bv
t_ε
XBL 738-1703

Fig. 2

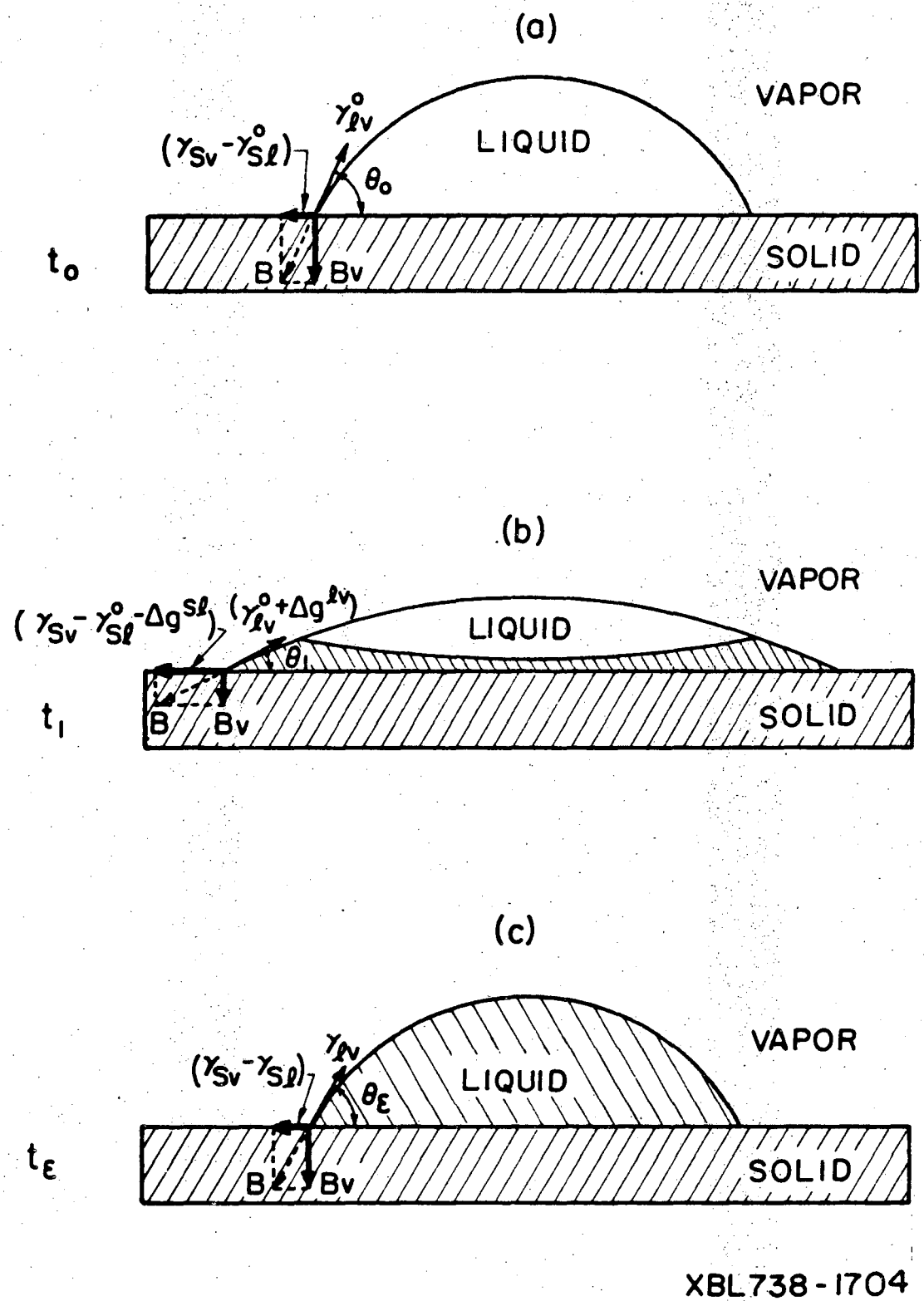
(a)
VAPOR
LIQUID
SOLID
$\gamma^o_{\ell v}$
$(\gamma_{Sv}-\gamma^o_{S\ell})$
θ_o
t_o
B
Bv
(b)
VAPOR
LIQUID
SOLID
$(\gamma_{Sv}-\gamma^o_{S\ell}-\Delta g^{S\ell})$
$(\gamma^o_{\ell v}+\Delta g^{\ell v})$
θ_1
t_1
B
Bv
(c)
VAPOR
LIQUID
SOLID
$\gamma_{\ell v}$
$(\gamma_{Sv}-\gamma_{S\ell})$
θ_ε
t_ε
B
Bv
XBL738-1704

Fig. 3

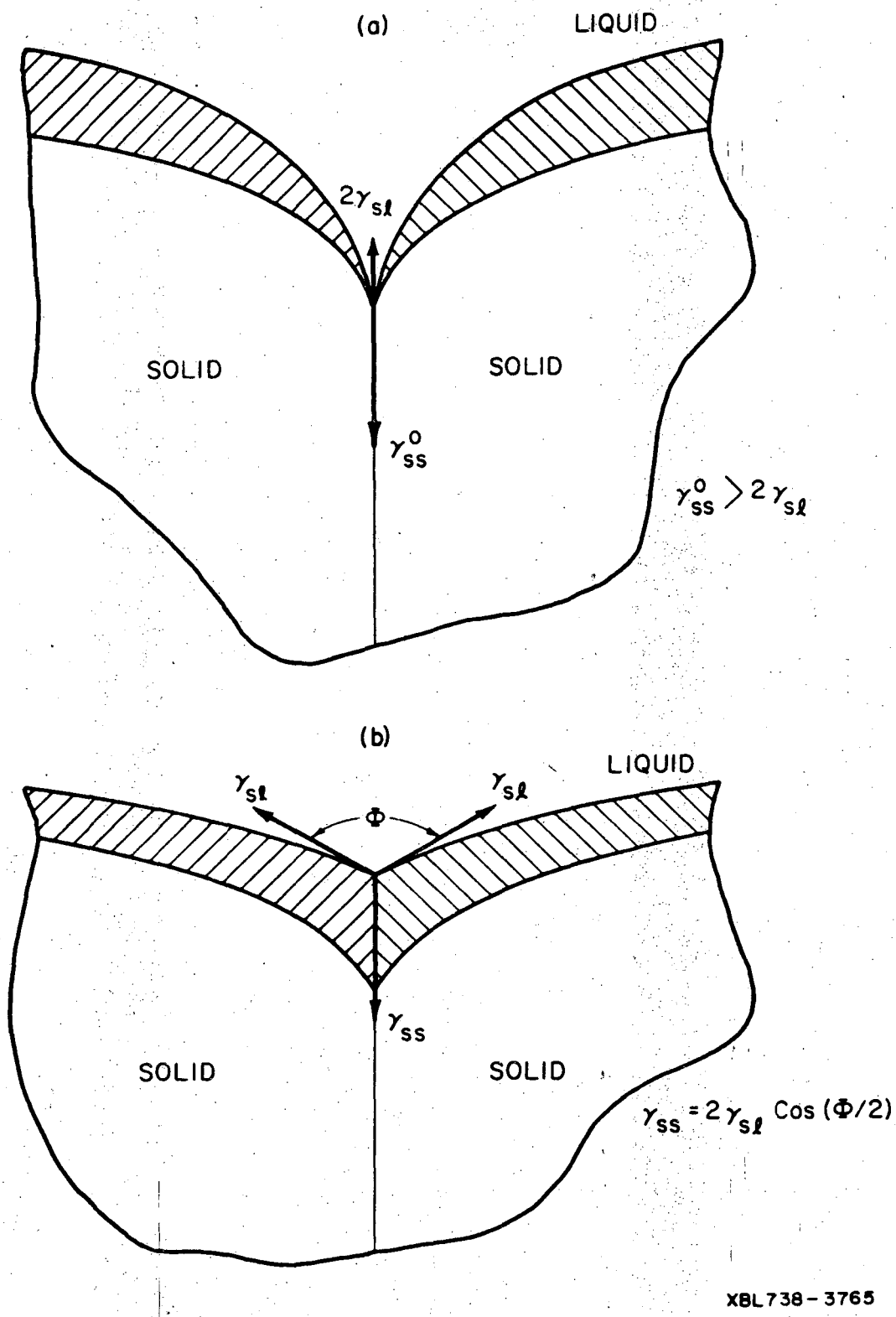
(a)
LIQUID
$2\gamma_{s\ell}$
SOLID
SOLID
γ^{o}_{ss}
$\gamma^{o}_{ss} > 2\gamma_{s\ell}$
(b)
LIQUID
$\gamma_{s\ell}$
$\gamma_{s\ell}$
Φ
γ_{ss}
SOLID
SOLID
$\gamma_{ss} = 2\gamma_{s\ell} \cos(\Phi/2)$
XBL738-3765

Fig. 4

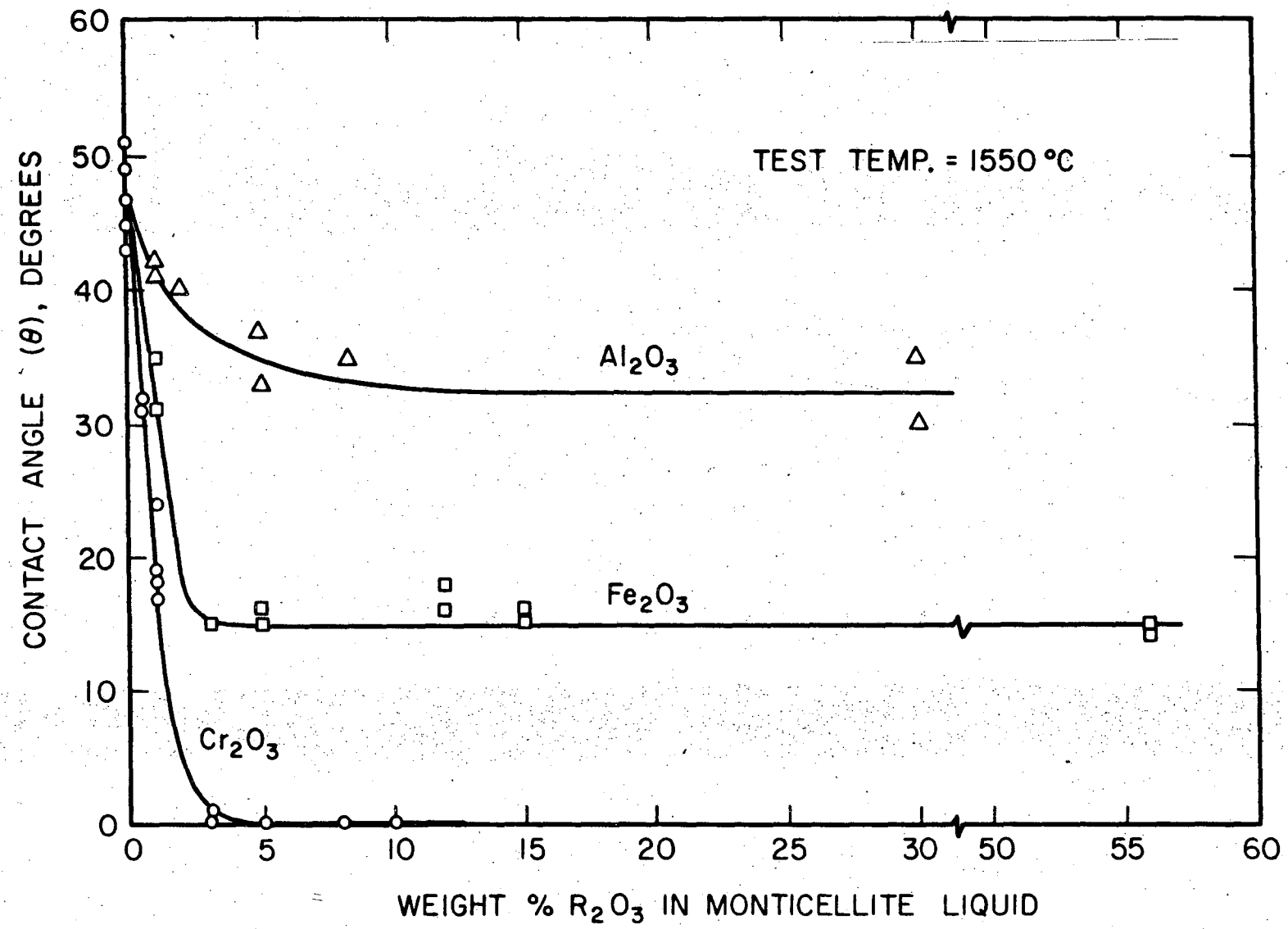

XBL 738 - 3766

Fig. 5

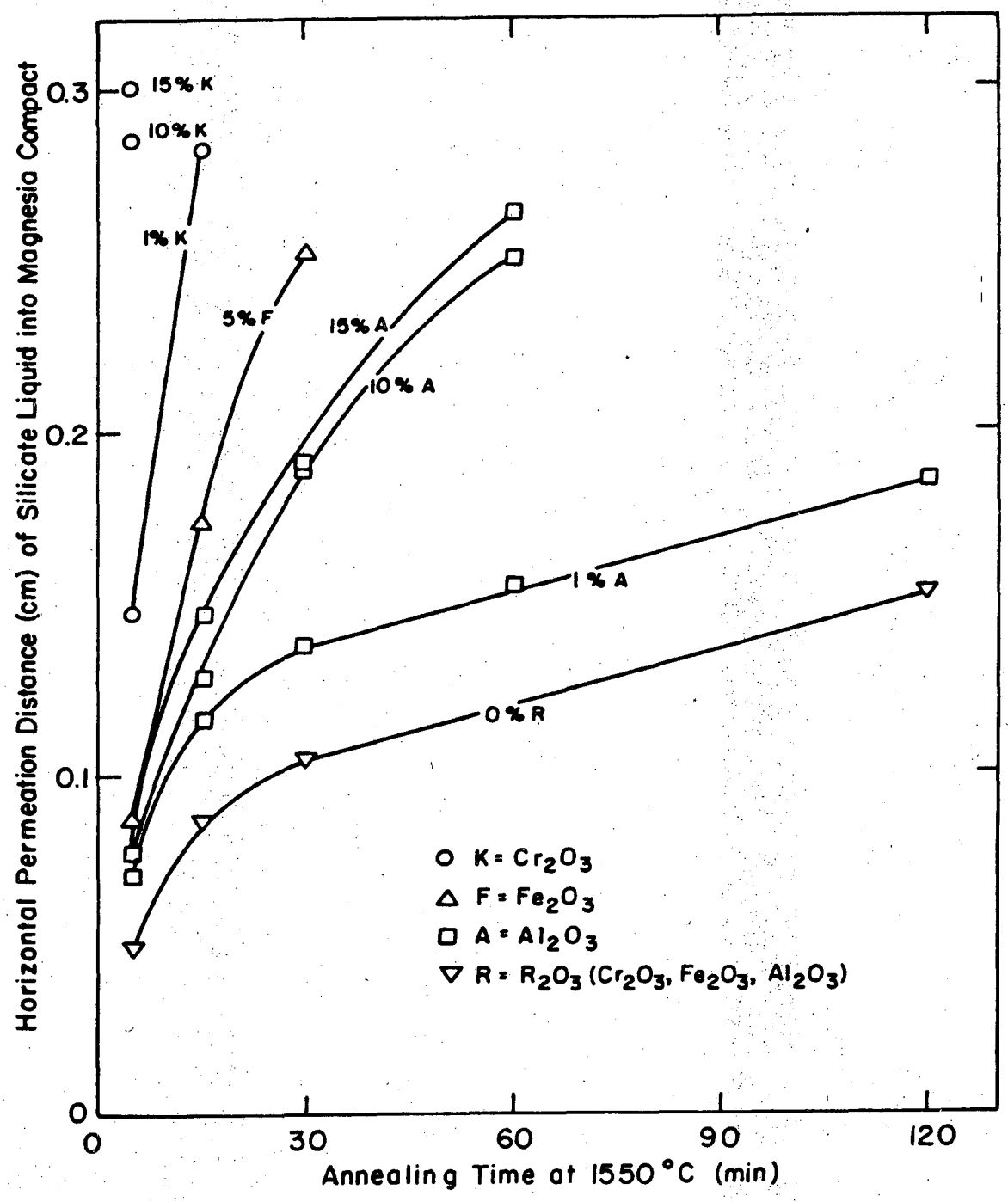

XBL 726-6365

Fig. 6

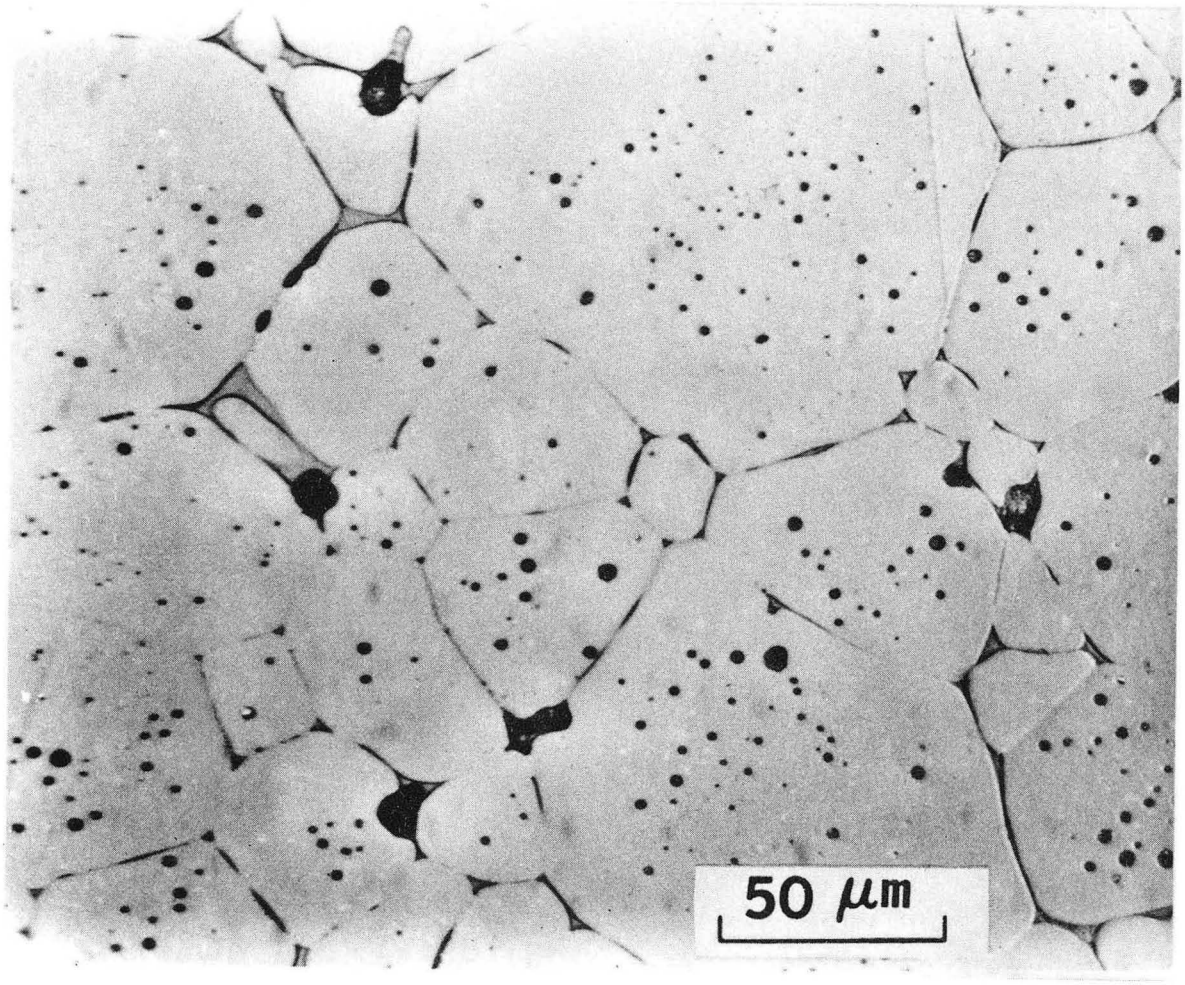

XBB 7210-5006

Fig. 7

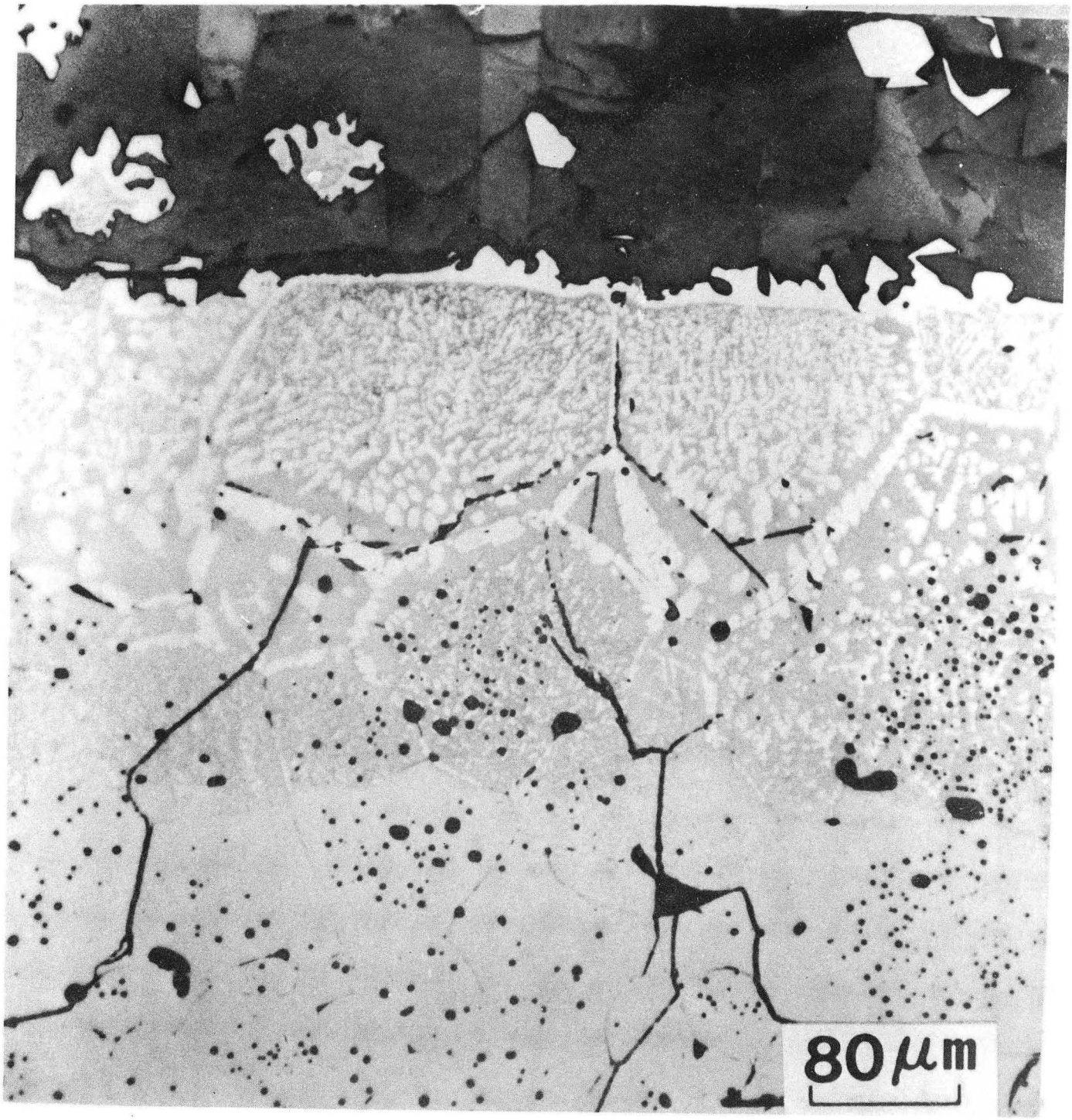

XBB 7210-5004 Bottom

Fig. 8

LEGAL NOTICE

This report was prepared as an account of work sponsored by the United States Government. Neither the United States nor the United States Atomic Energy Commission, nor any of their employees, nor any of their contractors, subcontractors, or their employees, makes any warranty, express or implied, or assumes any legal liability or responsibility for the accuracy, completeness or usefulness of any information, apparatus, product or process disclosed, or represents that its use would not infringe privately owned rights.

TECHNICAL INFORMATION DIVISION
LAWRENCE BERKELEY LABORATORY
UNIVERSITY OF CALIFORNIA
BERKELEY, CALIFORNIA 94720